

Magnetic domain structure of Fe–55 at.%Pd alloy at different stages of atomic ordering

Lisha Wang^{a)} and David E. Laughlin

Department of Materials Science and Engineering, Carnegie Mellon University, 5000 Forbes Avenue, Pittsburgh, Pennsylvania 15213

Y. Wang

Department of Materials Science and Engineering, The Ohio State University, 2041 College Road, Columbus, Ohio 43210

Armen G. Khachaturyan

Department of Ceramic and Materials Engineering, Rutgers University, 607 Taylor Road, Piscataway, New Jersey 08854

(Presented on 14 November 2002)

In this work, we use Lorentz microscopy imaging technique to study the magnetic domain structure of Fe–55 at.%Pd alloy at different stages of atomic ordering. The underlying microstructure is characterized by using conventional transmission electron microscopy. At low annealing temperature, a tweed microstructure is formed. The ordered c variants in the tweed microstructure align along $\{110\}$ plane traces. At higher annealing temperatures, a polytwinned structure is formed. The increase in the coercivity of the tweed structure is related to the density of magnetic macrodomain intersection with the tetragonal variants. After long time annealing, coarsened $L1_0$ grains are formed. Two types of magnetic domains are found in these coarsened grains. One is the “stripe” magnetic domain where the magnetization direction or the c axis of the $L1_0$ grain is perpendicular to the surface orientation. The other is “plate-like” magnetic domain; the magnetization direction of the $L1_0$ grain is found to be parallel to the specimen surface orientation.

© 2003 American Institute of Physics. [DOI: 10.1063/1.1541646]

I. INTRODUCTION

High uniaxial magnetocrystalline anisotropy K_u materials, such as Fe–Pd and Fe–Pt alloys, are attractive for ultra-high density magnetic recording and strong permanent magnet applications. The magnetic properties of these alloys are closely related to the microstructure of the tetragonal phase, which arises from the $A1 \rightarrow L1_0$ ordering.¹

It has been shown that during the atomic ordering, the alloy system develops a twinned microstructure to relieve the lattice mismatch strain.^{2,3} At different stages of atomic ordering in the FePd alloy, two microstructures can be easily identified, one is the tweed structure, and the other is polytwinned structure. A tweed microstructure arises from the ordered particles arranging themselves along certain directions to accommodate the elastic strain produced through the ordering process.⁴ The polytwinned microstructure appears at later stage of ordering; it contains a hierarchy of twin variants.⁵

At temperatures below the Curie temperature T_c , the ordered FePd alloy becomes ferromagnetic and each ordered $L1_0$ twin variant is a magnetic microdomain with the easy axis along the c axis. The magnetic domain structure of the equiatomic FePd polytwinned microstructure has been studied extensively in the literature and recently has been reviewed by Vlasova *et al.*¹ However, less work has been done to study the magnetic domain structure of nonequiatomic

Fe–Pd alloy, and magnetic domain structure of other microstructures, such as the tweed microstructure. The present investigation is aimed to characterize the magnetic domain structure of Fe–55 at.%Pd alloy at different stages of atomic ordering by using Lorentz microscopy and to relate the domain structure to the magnetic properties. The underlying crystallographic microstructure is also characterized by using conventional transmission electron microscopy (TEM).

II. EXPERIMENTS

The Fe–55 at.%Pd alloy used in this study was prepared by using the arc-melting process. The bulk Fe–Pd alloy was homogenized at 1113 K for 24 h and further annealed at two different temperatures, namely 773 and 663 K. The annealing time varied from 3 to 140 h. The detailed annealing temperature and time for each specimen is listed in Table I. All the thermal annealing experiments were carried out in evacuated quartz tubes back-filled with Ar gas. Thin foils for TEM observation were electropolished in a twinjet polisher using 25 V at 0 °C. The solution consisted of 82 vol.% gla-

TABLE I. The annealing conditions for Fe–55 at.%Pd.

Sample No.	Annealing temperature (K)	Time (h)
A	663	40
B	663	140
C	773	3
D	773	36

^{a)} Author to whom correspondence should be addressed; electronic mail: lisha@andrew.cmu.edu

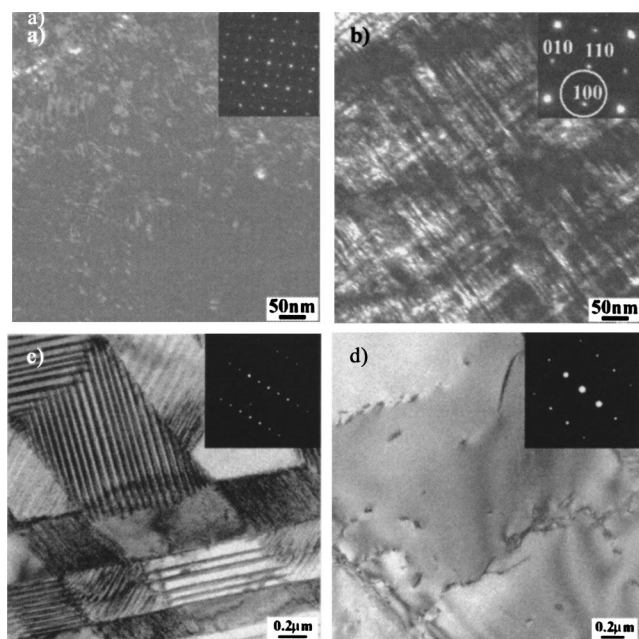


FIG. 1. Microstructure of Fe-55 at.%Pd after annealing: (a) and (b) are TEM bright field and dark field images of the tweed microstructure in specimen A. The inset diffraction pattern has the [001] zone axis. (c) and (d) TEM bright field image of polytwinned microstructure in specimen D. Inset diffraction pattern has the [130] zone axis. TEM bright field image of coarsened $L1_0$ grains in specimen D. Inset diffraction pattern has the [103] zone axis.

cial acetic acid, 9 vol.% perchloric acid, and 9 vol.% ethanol.⁵ Both conventional TEM and Lorentz microscopy were carried out in a JEOL 4000 microscope equipped with Gatan image filter. The magnetic properties were measured by using a vibrating sample magnetometer at room temperature.

III. RESULTS

X-ray diffraction (XRD) shows the splitting of (200) and (002) and (002), (311) and (113) peaks in all the alloys, indicating the change of the fcc structure to the $L1_0$ structure. In addition, if we assume that specimen D is a fully ordered specimen with order parameter equal to 1, we can estimate the order parameter for three other alloys by carefully choosing the superlattice peaks, $(001)_{L10}$ and $(110)_{L10}$ and the fundamental peaks $(002)_{L10}$ and $(220)_{L10}$, within the same family.⁶ The order parameters of specimen A, B, C, and D were calculated as 0.6, 0.9, 0.8, and 1, respectively.

The coercivity of these specimens is measured by using a vibrating sample magnetometer and the results are listed in

Table II. We find that the coercivity does not necessarily increase with the increment of the degree of the ordering. For the specimens annealed at both 773 and 663 K, the coercivity of Fe-55 at.%Pd are comparable to those of equiatomic FePd annealed at similar temperatures.⁵

From the TEM observations, it can be seen that the four specimens have different microstructures: specimen A has mainly a tweed microstructure [Figs. 1(a) and 1(b)], specimen B has both tweed and coarsened $L1_0$ grain structure specimen C has mainly polytwinned microstructure; specimen D has both the polytwinned microstructure [Fig. 1(c)] and coarsened $L1_0$ grains [Fig. 1(d)]. In addition to the three microstructures mentioned above, we found antiphase boundaries (APBs) in both specimens B and C. Therefore, the microstructure is the key factor in determining the extrinsic magnetic properties of these specimens. The microstructures of the four specimens are tabulated in Table II.

IV. DISCUSSION

In order to study the relationship between the magnetic properties and the microstructure, we use the Lorentz TEM imaging technique to observe the magnetic domain structures for each type of the microstructures.

Figures 2(a) and 2(b) show the magnetic domain wall images of a tweed microstructure formed in specimen A. The magnetic domains walls are imaged as alternate bright and dark lines, and the contrast of these lines changes when imaged from under-focus Fresnel mode to over-focus Fresnel mode. In these images, we observe both magnetic microdomains and magnetic macrodomains. The magnetic microdomain walls are coincident with the boundary of the finely dispersed plate shape c variants. Only two directions of the boundaries are present in these two micrographs. From the diffraction pattern [the inset of Fig. 1(a)], we can see that all the three types of $L1_0$ variants are present. The dark field image [Fig. 1(b)] clearly shows the tweed contrast along the {110} plane traces. The magnetic macrodomain walls pass through the boundaries of these c variants and each magnetic macrodomain wall intersects with a large number of magnetic microdomain walls.

Figure 2(c) shows the corresponding magnetic domain images for the same places as shown in Fig. 1(c). In these two figures, we can see the magnetic microdomain walls and macrodomain walls in the polytwinned structure. The magnetic microdomain walls coincide with the twin boundaries, and cannot move during the magnetization process. The magnetic macrodomain walls, however, have a zigzag shape; and they can be moved during the magnetization. The zigzag

TABLE II. The list of order parameter, coercivity, and microstructure of Fe-55at.%Pd alloy.

Sample	S_{order}	H_c (Oe)	Microstructure			
			Tweed	Polytwin	Coarsened $L1_0$ grain	APB
A	0.6	550	High %	None	Few	None
B	0.9	372	Medium %	None	Medium %	High density
C	0.8	155	Few	High %	Medium %	High density
D	1	100	None	Medium %	High %	None

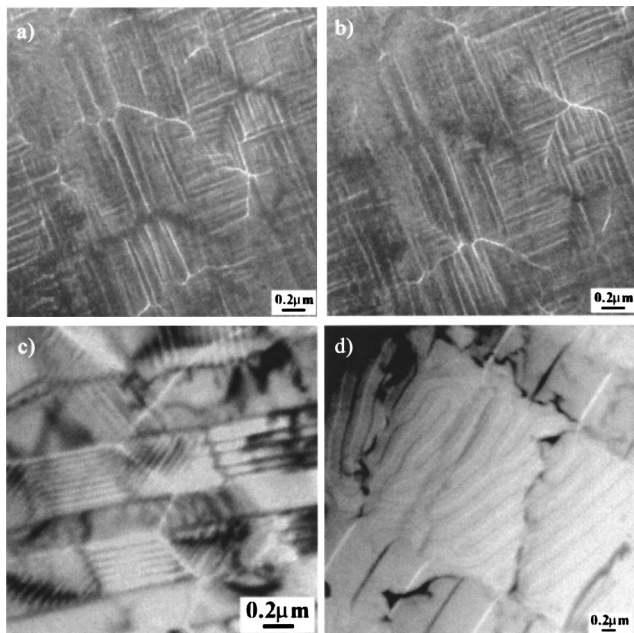


FIG. 2. The magnetic domain structure of Fe-55 at.%Pd after annealing. (a) and (b) are Lorentz under-focus and over-focus Fresnel image of tweed microstructure in specimen A. (c) Lorentz under-focus Fresnel image of polytwinned microstructure in specimen D. (d) Lorentz under-focus and Fresnel image of coarsened $L1_0$ grains in specimen D.

domain walls pass through the microtwin and macro twin variants, the directions of which are the combination of the magnetization directions of each microtwin variant.^{7,8}

Two types of magnetic domains are shown in Fig. 2(d) for coarsened $L1_0$ grains in Fig. 1(d). One is the stripe domain in the center grain; the other is the plate-like domains in outer side grains. By using the diffraction pattern to determine the surface orientation, we find the surface orientations in the center grain and side grains are $[0.28, 0.18, 1]$, $[1, 0.18, 0.35]$, respectively. That means that the magnetization direction in the center area is nearly perpendicular to the sample surface, therefore, it shows the characteristic “stripe” domain structure. On the other hand, the magnetization directions in the side regions are close to having the c axis of the grain in plane.

It has been suggested that the coercivity mechanism of the twinned Fe-Pd alloy is due to the wall pinning at the planar defects of $L1_0$ twin variants.¹ Comparing the magnetic domain structures of each type of the microstructures, we find that, in the tweed structure, the magnetic macrodomain walls have the strongest interaction with the c variants boundaries, because they intersect with the c -variant boundaries at very high density. During the magnetization, the magnetic macrodomain walls can be pinned at these intersections and hence the coercivity of the specimen is increased. The high coercivity in specimens A and B is due to their high density of tweed structures. This is consistent with the analysis in the literature.⁹ The twin boundaries in the polytwinned structure can also become the pinning sites for the domain walls, but they are not as effective as the c -variant boundaries in the tweed structure. This is because the magnetic macrodomain walls intersect with fewer mi-

cro twin variant boundaries and they can be easily moved inside the macro twin variants. In the coarsened $L1_0$ grains, the grain size is so large that there are many magnetic domains in one c variant. The domain wall can easily move or nucleate in the grains. Therefore the coercivity in these grains is relatively small.

V. CONCLUSION

In this work, we use a Lorentz microscopy imaging technique to study the magnetic domain structure and the underlying microstructure of Fe-55 at.%Pd alloy at different stages of atomic ordering. We find that Fe-55 at.%Pd annealed at 773 and 663 K gives similar coercivity compared with the equiatomic FePd heat treated at similar temperatures. We also identified three types of microstructures formed during the $A1 \rightarrow L1_0$ transformation, namely the tweed microstructure, the polytwinned microstructure, and the coarsened $L1_0$ grain microstructure.

It is found that in the tweed microstructure, all three $L1_0$ variants are present. These c variants align themselves along $\{110\}$ twin plane traces. The magnetic domain structure of this microstructure consists of two types of magnetic domain walls: one is the magnetic microdomain wall along the $\{110\}$ c -variant boundary; the other is the magnetic macrodomain wall that runs across many c -variant boundaries. There are also magnetic micro- and macrodomain walls appearing in the polytwinned microstructure. We attribute the higher coercivity of the tweed structure to the higher density of the intersection between the macrodomain walls and the c variants.

In the coarsened $L1_0$ grain microstructure, we also observe the magnetic domain structures within one grain. Depending on the magnetization direction of the grain, there are two types of magnetic domains: “stripe” domains if the magnetization direction is perpendicular to the surface orientation; and “plate-like” domains if the magnetization direction is parallel to the surface orientation.

ACKNOWLEDGMENTS

The authors would like to thank Professor Soffa at University of Pittsburgh for his helpful discussions and N. T. Nuhfer for help with Lorentz imaging. This work is supported by National Science Foundation under Grant No. DMR-9905723.

¹N. I. Vlasova, G. S. Kandaurova, and N. N. Shchegoleva, *Fiz. Met. Metalloved.* **90**, 31 (2000).

²G. M. Gushchin and F. N. Berseneva, *Fiz. Met. Metalloved.* **63**, 926 (1987).

³L. Q. Chen, Y. Wang, and A. G. Khachatryan, *Philos. Mag. Lett.* **65**, 15 (1992).

⁴A. G. Khachatryan, *Theory of Structural Transformations in Solids* (Wiley, New York, 1983).

⁵B. Zhang and W. A. Soffa, *Phys. Status Solidi A* **131**, 707 (1992).

⁶N. D. Zemtsova and A. Yu. Sokolova, *Fiz. Met. Metalloved.* **82**, 186 (1996).

⁷L. Wang, Z. Fan, and D. E. Laughlin, *Scr. Mater.* **47**, 781 (2002).

⁸A. Kazaryan, Y. Wang, Y. M. Jin, Y. U. Wang, A. G. Khachatryan, L. Wang, and D. E. Laughlin, *J. Appl. Phys.* (to be published).

⁹T. Klemmer, D. Hoydick, H. Okumura, B. Zhang, and W. A. Soffa, *Scr. Metall. Mater.* **33**, 1793 (1995).